



RIETI Discussion Paper Series 25-E-055

Quantifying Congestion Externalities in Road Networks: A structural estimation approach using stochastic evolutionary model

FUJISHIMA, Shota
Hitotsubashi University

SAKAI, Takara
Institute of Science Tokyo

TAKAYAMA, Yuki
Institute of Science Tokyo



The Research Institute of Economy, Trade and Industry
<https://www.rieti.go.jp/en/>

Quantifying Congestion Externalities in Road Networks: A structural estimation approach using stochastic evolutionary model*

Shota Fujishima

Graduate School of Economics, Hitotsubashi University

Takara Sakai

School of Environment and Society, Institute of Science Tokyo

Yuki Takayama

Department of Civil and Environmental Engineering, Institute of Science Tokyo

Abstract

This study estimates the structural parameters of a travel time function, which relates traffic volume to travel time, within the context of a traffic assignment model in which travelers strategically select routes to minimize their travel costs, influenced by congestion. The proposed model is formulated as a potential game, enabling the estimation of parameters using the maximum likelihood method based on a stochastic evolutionary process. The impact of congestion pricing on welfare is evaluated using the estimated parameters. Preliminary analysis using the Sioux Falls network shows that congestion pricing enhances overall welfare, even when accounting for estimation errors.

Keywords: road network, congestion, potential game, evolutionary game theory

JEL classification: R41, R48

The RIETI Discussion Paper Series aims at widely disseminating research results in the form of professional papers, with the goal of stimulating lively discussion. The views expressed in the papers are solely those of the author(s), and neither represent those of the organization(s) to which the author(s) belong(s) nor the Research Institute of Economy, Trade and Industry.

*This study was conducted as a part of the project “Evidence-Based Policy Making for Regional Revitalization” undertaken at the Research Institute of Economy, Trade and Industry (RIETI). We would like to thank participants of the RIETI DP Seminar for their helpful comments. This work was supported by Fusion Oriented Research for Disruptive Science and Technology (Grant No. JPMJFR215M), the Council for Science, Technology and Innovation (Grant No. JPJ012187), and JSPS KAKENHI (Grant Nos. 22K18525, 23K22880, 24K22973, and 25K01339). We also wish to thank Yusuke Hara, Daisuke Oyama, and Yuki Oyama, as well as the participants of the 2024 Applied Regional Science Conference and the 2025 Spring Meeting of the Japanese Economic Association, for their helpful comments and valuable feedback.

1 Introduction

Numerous urban areas encounter significant traffic congestion issues, which typically result in frustrating delays for commuters and increased pollution levels that adversely affect the overall quality of life for residents and the efficiency of local economies. To solve the pervasive and complex problem of road traffic congestion, it is essential to measure the external costs associated with congestion and require road users to fairly bear the corresponding expenses that arise from their travel behaviors and choices. To achieve this important goal, the travel cost functions that connect traffic volume to the associated travel expenses incurred by individuals as they navigate through the increasingly crowded roadways of cities should be evaluated.

In this study, we estimate the structural parameters of a travel time function that connects traffic volume to travel time given the equilibrium state of the model describing the traffic assignment over a road network. In this model, there exist a specific number of travelers for each origin and destination (OD) pair. Typically, multiple routes link an origin to a destination, and travelers select a route aimed at minimizing their travel expenses. Their travel expenses are influenced by congestion: the cost of travel increases with the number of travelers using the same road. Our approach is structured as a population game, in which the payoff relies solely on the distribution of the population over the available strategies (or routes chosen) rather than on the strategies of individual players. Consequently, our focus is on the Nash equilibrium.

Our game exclusively produces negative externalities; thus, the Nash equilibrium outcome is unique as long as the players are homogeneous. Furthermore, our traffic assignment problem falls into the category of *potential games* (Rosenthal, 1973; Monderer and Shapley, 1996), where determining the Nash equilibrium is simplified into determining the maximizer of a function referred to as the potential function.

In addition, we use the potential function to estimate the structural parameters. To derive the likelihood function, we consider a stochastic evolutionary process in which players gradually modify their strategies. More specifically, during each time period, one traveler receives an opportunity for revision. The traveler selects an opponent at random who has the same OD pair as he does and follows that opponent's route based on the *imitative exponential protocol* (Sandholm, 2010), where the likelihood of switching increases with the opponent's payoff. This procedure is structured as a Markov chain; thus, its stationary distribution, which is considered as the likelihood function, relies solely on states via the potential function.

The potential function method is extensively recognized in the field of structural estimation for network games (e.g., Nakajima, 2007; Mele, 2017; Hsieh et al., 2022). As noted by Mele (2017), calculating the normalizing constant of the stationary distribution, which ensures that the distribution totals 1, is challenging because it requires summing the values across all possible states. Mele (2017) used a Bayesian strategy that uses an advanced version of the Metropolis-Hasting algorithm to circumvent the direct calculation of the normalizing constant.

In contrast, we note that the log-likelihood function converges regarding the number of players, and in the context of our road traffic assignment issue, this figure can be regarded as substantial. In the limit function, the task of calculating the normalizing constant is substituted with the maximization of the potential function. Although maximizing a function can also be generally challenging, our limit function is strictly concave because our game includes only negative externalities. Therefore, we substitute the likelihood function with its limit counterpart as an approximation and estimate the parameters using the maximum likelihood method. The standard errors of the maximum likelihood estimates are derived using the bootstrap technique.

We use the Bureau of Public Roads (BPR) function, which is commonly used in transportation modeling and practical evaluations of transportation (e.g., Sheffi, 1985; Small et al., 2024) for the travel time function, and estimate its parameters using the maximum likelihood approach, where the likelihood function is approximated under the assumption that the number of travelers is sufficiently large. For preliminary analysis, we use artificial observation data from a test network referred to as the Sioux Falls network, which comprises 24 nodes and 76 links. The results indicate that the parameters are estimated efficiently, with their standard errors derived using the bootstrap technique. Furthermore, we assess the congestion externalities based on the estimated parameters and evaluate the welfare gains resulting from link-based congestion pricing, which theoretically attains the optimal allocation. We find that the variability of welfare improvements from the link-based congestion pricing is relatively minimal, indicating that the adoption of such pricing strategies results in predictable enhancements in overall network efficiency, thereby improving the economic welfare of users while successfully addressing congestion.

Addressing traffic congestion is a critical policy challenge; thus, it has received significant attention in the fields of transportation and urban studies. Viauoux (2011) explored a model in which travelers determine both the number of trips they take and their mode of transportation. All travelers have the same origin and destination. He used data from a household survey conducted in Montpellier, France. He discovered notable enhancements in overall welfare when marginal cost pricing was applied. Durrmeyer and Martinez (2022) examined a model in which travelers select their departure times and modes of transportation, with predefined routes. Using commuting data from Paris, the authors investigated the effects of different road pricing and transit frequency adjustment scenarios on different income groups. Almagro et al. (2024) analyzed a model in which travelers select their mode of transportation. The authors posited that routes are predetermined, because travelers follow the directions provided by Google Maps. Using traffic data from community areas in Chicago, they found that road pricing can significantly reduce externalities while improving the quality of public transit service. The authors also examined the distributional effects of different road pricing and transit frequency adjustment scenarios on different income groups. All aforementioned studies used the discrete choice method to estimate the structural parameters.

Although these studies consider elements that are not addressed in the present study, such as various transportation modes and the diversity among travelers, they do not consider the route choices made by road users.¹ This neglect may result in issues because travelers may re-evaluate their route choices due to anticipated traffic disruptions, such as scheduled construction. Disregarding route selection can result in imprecise forecasts of traffic patterns and congestion levels, because travelers may opt for different routes to circumvent delays. In addition, the adjustments travelers make in response to transportation policies, such as congestion pricing, can significantly affect overall traffic flow and congestion levels, which are essential for formulating effective transportation policies.

This paper is organized as follows. Section 2 presents the model and introduces the potential game approach. Section 3 presents an estimation method that uses the potential function and reports the preliminary results from a toy dataset. Section 4 discusses congestion pricing for optimal traffic assignment and evaluates the variability in the welfare gains resulting from congestion pricing. Section 5 concludes the study. The details of the dataset and numerical algorithm, along with the omitted proofs, are provided in the appendix.

2 Model

2.1 Basic assumptions

We consider a model in which agents select their routes in a transportation network. The network is represented as a directed graph consisting of a set of nodes \mathcal{N} and a set of links \mathcal{L} . Let $\mathcal{R} \subseteq \mathcal{N}$ denote the set of origin nodes from which agents depart, and let $\mathcal{S} \subseteq \mathcal{N}$ denote the set of destination nodes at which agents arrive. Each OD pair $(r, s) \in \Omega \equiv \mathcal{R} \times \mathcal{S}$ is connected by a set of paths (routes) \mathcal{K}^{rs} through the network. A path $k \in \mathcal{K}^{rs}$ for an OD pair (r, s) is a sequence of links connecting origin $r \in \mathcal{R}$ to destination $s \in \mathcal{S}$.

A link from node $i \in \mathcal{N}$ to node $j \in \mathcal{N}$ is denoted as link (i, j) . The travel cost for traversing link (i, j) depends solely on the traffic flow rate y_{ij} on the link. We assume that the travel cost function $t_{ij}(y_{ij})$ for link (i, j) is nonnegative, continuously differentiable, strictly increasing, and convex, as commonly assumed in the literature (e.g., Sheffi, 1985; Fajgelbaum and Schaal, 2020; Allen and Arkolakis, 2022). This implies that high traffic flow causes increased delays on the link due to congestion.

All agents are homogeneous and select a path to minimize their travel costs from an origin to a destination. The total number of agents in the network is fixed and denoted by Q ; we

¹In the quantitative spatial economics (QSE) literature, there are some papers that address both congestion and route choice. Fajgelbaum and Schaal (2020) consider the route choice problem in the transportation sector, which is faced with congestion during the shipping of goods. Their focus is on the optimal allocation. Allen and Arkolakis (2022) examine a routing framework within an urban model where individuals travel from their residences to their workplaces. By utilizing a dataset of the Seattle road network, they assess the welfare elasticity resulting from enhancements to the road network and the associated return on investment. In contrast to the QSE literature, our ultimate goal is statistical inference of structural parameters.

assume it is large but finite: $Q \in \mathbb{N}$. Let $q_Q^{rs} \in \frac{1}{Q}\mathbb{Z}_+$ be the proportion of agents with OD pair (r, s) , which are referred to as agents (r, s) . Then, the total number of agents (r, s) is Qq^{rs} , and $\sum_{(r,s) \in \Omega} q^{rs} = 1$. In addition, let $f_{Qk}^{rs} \in \frac{1}{Q}\mathbb{Z}_+$ denote the proportion of agents (r, s) selecting path $k \in \mathcal{K}^{rs}$, satisfying $\sum_{k \in \mathcal{K}^{rs}} f_{Qk}^{rs} = q_Q^{rs}$. Then, the traffic flow rate $y_{ij} \in \mathbb{R}_+$ on link (i, j) is expressed as follows:

$$y_{ij}(\mathbf{f}_Q) = \sum_{(r,s) \in \Omega} \sum_{k \in \mathcal{K}^{rs}} f_{Qk}^{rs} \delta_{ij,k}^{rs}, \quad (1a)$$

$$\delta_{ij,k}^{rs} = \begin{cases} 1 & \text{if link } (i, j) \text{ is part of path } k \in \mathcal{K}^{rs}, \\ 0 & \text{otherwise,} \end{cases} \quad (1b)$$

where $\mathbf{f}_Q = (f_{Qk}^{rs})_{k \in \mathcal{K}^{rs}, (r,s) \in \Omega}$. Using matrix notation, (1) can be rewritten as follows:

$$\mathbf{y}(\mathbf{f}_Q) = \Delta \mathbf{f}_Q, \quad (2)$$

where $\mathbf{y}(\mathbf{f}_Q) = (y_{ij}(\mathbf{f}_Q))_{(i,j) \in \mathcal{L}}$ and Δ denotes the path-link incidence matrix with elements $\delta_{ij,k}^{rs}$.

The travel cost C_k^{rs} for a path $k \in \mathcal{K}^{rs}$ is the sum of the costs of the links that form path k . Therefore, C_k^{rs} can be expressed as a function of \mathbf{f}_Q as follows:

$$C_k^{rs}(\mathbf{f}_Q) = \sum_{(i,j) \in \mathcal{L}} t_{ij}(y_{ij}(\mathbf{f}_Q)) \delta_{ij,k}^{rs}. \quad (3)$$

2.2 Equilibrium and potential game

Our model can be considered a finite-population congestion game (Rosenthal, 1973), where the set of populations is denoted by Ω , the action set is \mathcal{K}^{rs} , and the population state is an element of $\mathcal{F}_Q \equiv \prod_{(r,s) \in \Omega} \mathcal{F}_Q^{rs}$, with

$$\mathcal{F}_Q^{rs} = \left\{ \mathbf{f}_Q^{rs} \in \mathbb{R}_+^{|\mathcal{K}^{rs}|} \cap \frac{1}{Q}\mathbb{Z}_+^{|\mathcal{K}^{rs}|} \mid \sum_{k \in \mathcal{K}^{rs}} f_{Qk}^{rs} = q_Q^{rs} \right\}, \quad (4)$$

where $\mathbf{f}_Q^{rs} = (f_{Qk}^{rs})_{k \in \mathcal{K}^{rs}}$. The payoff function is $\boldsymbol{\pi}(\mathbf{f}_Q) = (\pi_k^{rs}(\mathbf{f}_Q))_{k \in \mathcal{K}^{rs}, (r,s) \in \Omega}$, where $\pi_k^{rs}(\mathbf{f}_Q) = -C_k^{rs}(\mathbf{f}_Q)$. Following Sandholm (2010, 2015), we identify a game by its payoff function $\boldsymbol{\pi}$; thus, we denote our game by $\boldsymbol{\pi}$.

The Nash equilibrium² of game $\boldsymbol{\pi}$ is the state in which no agent can gain by changing their path, meaning that they have no incentive to switch to another path. Formally, $\mathbf{f}_Q^* \in \mathcal{F}_Q$ is

²In the field of transportation, the Nash equilibrium of congestion games is commonly referred to as the user equilibrium.

an equilibrium if, for all $(r, s) \in \Omega$, the following condition holds

$$f_{Qk}^{rs*} > 0 \implies \pi_k^{rs}(\mathbf{f}_Q^*) \geq \pi_\ell^{rs} \left(\mathbf{f}_Q^* + \frac{1}{Q}(\mathbf{e}_\ell^{rs} - \mathbf{e}_k^{rs}) \right) \quad \forall k, \ell \in \mathcal{K}^{rs}, \quad (5)$$

where \mathbf{e}_k^{rs} denotes the unit vector with a value of one in the position corresponding to $k \in \mathcal{K}^{rs}$.

We use the properties of a *potential game* to characterize the equilibrium and estimate the parameters of our model. A game is called a potential game if there exists a potential function p_Q that satisfies

$$p_Q(\mathbf{f}_Q) - p_Q \left(\mathbf{f}_Q - \frac{1}{Q} \mathbf{e}_k^{rs} \right) = \pi_k^{rs}(\mathbf{f}_Q) \quad \forall \mathbf{f}_Q \in \mathcal{F}_Q, \quad \forall k \in \mathcal{K}^{rs}, \quad \forall (r, s) \in \Omega. \quad (6)$$

As reported in Rosenthal (1973) and Monderer and Shapley (1996), every congestion game is a potential game with the following potential function

$$p_Q(\mathbf{f}_Q) = - \sum_{(i,j) \in \mathcal{L}} \sum_{z=1}^{Qy_{ij}(\mathbf{f}_Q)} t_{ij} \left(\frac{z}{Q} \right). \quad (7)$$

The potential function (7) satisfies (6) in our model. Thus, our game π is a finite-population potential game.

To estimate the parameters of our model, we consider a game in which the total number of agents approaches infinity (i.e., $Q \rightarrow \infty$), which we call a continuum-population game. The population state of our continuum-population game is an element of $\mathcal{F} \equiv \prod_{(r,s) \in \Omega} \mathcal{F}^{rs}$, with

$$\mathcal{F}^{rs} = \left\{ \mathbf{f}^{rs} \in \mathbb{R}_+^{|\mathcal{K}^{rs}|} \mid \sum_{k \in \mathcal{K}^{rs}} f_k^{rs} = q^{rs} \right\}, \quad (8)$$

where $q^{rs} \in \mathbb{R}_+$ denotes the proportion of agents (r, s) . As demonstrated in Sandholm (2001), continuum-population potential games are the limits of convergent sequences of finite-population potential games. This implies that our continuum-population game admits a potential function $p(\cdot)$, as shown in the following lemma:

Lemma 1 *For all $\epsilon > 0$, there exists Q such that*

$$\left| \frac{1}{Q} p^Q(\mathbf{f}_Q) - p(\mathbf{f}_Q) \right| \leq \epsilon \quad \forall \mathbf{f}_Q \in \mathcal{F}_Q, \quad (9)$$

where the potential function $p(\mathbf{f}_Q)$ is given by

$$p(\mathbf{f}_Q) = - \sum_{(i,j) \in \mathcal{L}} \int_0^{y_{ij}(\mathbf{f}_Q)} t_{ij}(z) dz. \quad (10)$$

Proof See Appendix C.1.

The equilibrium of a continuum-population potential game is characterized by its potential function. Specifically, the state $\mathbf{f}^* \in \mathcal{F}$ is an equilibrium of our game π if and only if it is a Karush–Kuhn–Tucker (KKT) point for the maximization problem of the potential function.

$$\max_{\mathbf{f} \in \mathcal{F}} p(\mathbf{f}). \quad (11)$$

Therefore, we investigate the uniqueness of the equilibrium by checking the shape of the potential function. The following proposition establishes uniqueness for the link flow rate but not for the population state.

Proposition 1 *In the continuum-population game π , the equilibrium link flow rate $\mathbf{y}(\mathbf{f}^*) = (y_{ij}(\mathbf{f}^*))_{(i,j) \in \mathcal{L}}$ is uniquely determined, whereas the equilibrium population state \mathbf{f}^* is generally non-unique.*

Proof See Appendix C.2.

Each agent’s path choice, represented by \mathbf{f} , determines the traffic flow rate on each link $y_{ij}(\mathbf{f})$. Although the potential function $p(\mathbf{f})$ initially appears to depend on individual path choices, it is governed by the aggregate link flow rates $\mathbf{y}(\mathbf{f})$. Therefore, $p(\mathbf{f})$ can be redefined as $g(\mathbf{y}(\mathbf{f}))$, where aggregate link flow rates (rather than individual paths) influence the potential:

$$g(\mathbf{y}) = - \sum_{(i,j) \in \mathcal{L}} \int_0^{y_{ij}} t_{ij}(z) dz. \quad (12)$$

Proposition 1 is obtained because the Hessian matrix $\nabla^2 g(\mathbf{y})$ is negative definite (i.e., $g(\mathbf{y})$ is strictly concave), whereas $\nabla^2 p(\mathbf{f})$ is not.

Numerical analysis and parameter estimation for our model require defining the population state \mathbf{f} , which necessitates enumerating all paths available within the network. However, enumerating all possible paths in large networks is infeasible because of the extensive number of potential routes. To address this issue, we reformulate the maximization problem in (11) to eliminate the need for explicit path enumeration. Specifically, we decompose (11) into a problem that consists only of link flow rates by each origin, denoted by $\mathbf{x} = (x_{ij}^r)_{(i,j) \in \mathcal{L}, r \in \mathcal{R}} \in \mathbb{R}_+^{|\mathcal{L} \times \mathcal{R}|}$, where x_{ij}^r denotes the flow rate on link (i, j) for agents with origin r .

$$\max_{\mathbf{x} \in \mathbb{R}_+^{|\mathcal{L} \times \mathcal{R}|}} g(\hat{\mathbf{y}}(\mathbf{x})) = - \sum_{(i,j) \in \mathcal{L}} \int_0^{\hat{y}_{ij}(\mathbf{x})} t_{ij}(w) dw \quad (13a)$$

$$\text{s.t.} \quad \sum_{j \in \mathcal{N}^{\text{IN}}(i)} x_{ji}^r - \sum_{j \in \mathcal{N}^{\text{OUT}}(i)} x_{ij}^r = \begin{cases} - \sum_{s \in \mathcal{S}} q^{rs} & \text{if } i = r \\ q^{ri} & \text{if } (r, i) \in \Omega \\ 0 & \text{otherwise} \end{cases} \quad \forall i \in \mathcal{N}, \forall r \in \mathcal{R}, \quad (13b)$$

where $\mathcal{N}^{\text{IN}}(i)$ and $\mathcal{N}^{\text{OUT}}(i)$ denote the sets of nodes connected to and from node i by a link, respectively. The link flow rate $\hat{\mathbf{y}}(\mathbf{x}) = (\hat{y}_{ij}(\mathbf{x}))_{(i,j) \in \mathcal{L}}$ is given by

$$\hat{y}_{ij}(\mathbf{x}) = \sum_{r \in \mathcal{R}} x_{ij}^r. \quad (14)$$

The constraint (13b) enforces flow conservation at each node $i \in \mathcal{N}$, specifically for flow rates originating from $r \in \mathcal{R}$. This means that flow rates with origin r entering and exiting each node i are independently balanced. At the origin node r (i.e., $i = r$), the constraint permits a net outflow equal to the total demand originating from r . At destination nodes (i.e., $(r, i) \in \Omega$), the constraint allows a net inflow matching the demand arriving from origin r . For intermediate nodes that are neither origin r nor destinations, the inflow and outflow with origin r must match. This formulation accurately captures the distribution of flow across links for each OD pair.

Note that the two problems (11) and (13) provide the same link flow rates as proven in the following lemma:

Lemma 2 *The solution \mathbf{x}^* of (13) provides the unique link flow rate $\hat{\mathbf{y}}(\mathbf{x}^*) = (\hat{y}_{ij}(\mathbf{x}^*))_{(i,j) \in \mathcal{L}}$, which is equivalent to the equilibrium link flow rate $\mathbf{y}(\mathbf{f}^*)$ obtained from (11).*

Proof See Akamatsu (1997).

This reformulation allows us to efficiently obtain the unique equilibrium link flow rate \mathbf{y} by solving (13), thereby facilitating analysis and estimation even for complex, large networks.

3 Estimation

In this section, we estimate the link cost function $t_{ij}(\cdot)$. This function is critical for determining the travel costs associated with each link in the network, allowing us to analyze the effects of changes in traffic patterns and demand on overall route efficiency. We adopt the following parametric representation, known as the BPR function (U.S. Bureau of Public Roads, 1964):

$$t_{ij}(y_{ij}) = \bar{t}_{ij} \left(1 + \alpha \left(\frac{y_{ij}}{\mu_{ij}} \right)^\beta \right) \quad \forall (i, j) \in \mathcal{L}, \quad (15)$$

where \bar{t}_{ij} denotes the free-flow travel time on link (i, j) , μ_{ij} denotes the link capacity, and α and β are parameters.

The BPR function, with commonly applied values of $\alpha = 0.15$ and $\beta = 4.0$, is extensively used in transportation modeling and practical transportation evaluations (e.g., Sheffi, 1985; Small et al., 2024), even though equilibrium link flows under this specification may not always align with observed data. Given data of $\{y_{ij}, \mu_{ij}, \bar{t}_{ij}\}_{(i,j) \in \mathcal{L}}$ and $\{Q^{rs}\}_{(r,s) \in \Omega}$, where Q^{rs} denotes the total travel demand for the OD pair $(r, s) \in \Omega$, we estimate the parameter $\theta \equiv (\alpha, \beta)$ that is assumed to be common to all links.

3.1 Data

As a preliminary analysis, we conduct a numerical test on the proposed method below in which the true value of θ is known and set to $\theta = (0.15, 4.0)$ using the Sioux Falls network dataset provided by Transportation Networks for Research Core Team (Accessed: September 22, 2024). The Sioux Falls network consists of 24 nodes and 76 links (Figure 1). This dataset includes the capacity pattern $\boldsymbol{\mu} \equiv \{\mu_{ij}\}_{(i,j) \in \mathcal{L}}$, the free flow travel time pattern $\bar{\boldsymbol{t}} \equiv \{\bar{t}_{ij}\}_{(i,j) \in \mathcal{L}}$, and the OD demand pattern $\boldsymbol{Q} \equiv \{Q^{rs}\}_{(r,s) \in \Omega}$.³ The dataset also includes the Nash equilibrium link flow $\boldsymbol{v} \equiv \{v_{ij}\}_{(i,j) \in \mathcal{L}}$ when $\theta = (0.15, 4.0)$.⁴ Figure 2 shows the Nash equilibrium link flow \boldsymbol{v} . The details of the Sioux Falls network dataset are shown in Appendix B.

3.2 Method

3.2.1 Likelihood function

To establish the likelihood function, we consider a stochastic evolutionary process in which players gradually adjust their strategies. This approach is organized as a Markov chain, where its stationary distribution serves as the likelihood function. Formally, let $\{F_Q^t\}_{t \geq 0}$ be a Markov chain over \mathcal{F}_Q . Each player receives a revision opportunity based on an independent Poisson process with a rate of 1. Collectively, revision opportunities for players follow a Poisson process

³The OD demand Q^{rs} is related to q^{rs} by $Q^{rs} = Qq^{rs}$ where $Q = \sum_{(r,s) \in \Omega} Q^{rs}$.

⁴The link flow v_{ij} is related to the link flow rate y_{ij} by $v_{ij} = Qy_{ij}$.

with rate Q , meaning that the expected duration for which the economy remains in a given state is $1/Q$.

When an agent receives a revision opportunity, the agent updates its path according to the *imitative logit protocol* with noise level $\eta > 0$ (Sandholm, 2010, Section 11.5.2).⁵ The protocol operates as follows: Suppose an agent (r, s) currently following path $k \in \mathcal{K}^{rs}$ receives a revision opportunity. Then, the agent switches to path $\ell \in \mathcal{K}^{rs}$ with the following probability:

$$\frac{\rho_{k\ell}^{rs}(\mathbf{f}_Q) \exp[\eta^{-1} \pi_\ell^{rs}(\mathbf{f}_Q + \frac{1}{Q}(\mathbf{e}_\ell^{rs} - \mathbf{e}_k^{rs}))]}{\sum_{m \in \mathcal{K}^{rs}} \rho_{km}^{rs}(\mathbf{f}_Q) \exp[\eta^{-1} \pi_m^{rs}(\mathbf{f}_Q + \frac{1}{Q}(\mathbf{e}_m^{rs} - \mathbf{e}_k^{rs}))]}, \quad (16)$$

where

$$\rho_{k\ell}^{rs}(\mathbf{f}_Q) = \begin{cases} \frac{Q f_{Q\ell}^{rs} + 1}{Q q^{rs} + |\mathcal{K}^{rs}| - 1} & \text{if } \ell \neq k, \\ \frac{Q f_{Qk}^{rs}}{Q q^{rs} + |\mathcal{K}^{rs}| - 1} & \text{if } \ell = k. \end{cases} \quad (17)$$

$\rho_{k\ell}^{rs}(\mathbf{f}_Q)$ denotes the probability that an agent (r, s) taking path $\ell \in \mathcal{K}^{rs}$ is selected as an opponent of the revising player. In addition to the Q agents, one committed agent is assumed to exist for each path. This explains the addition of 1 to $Q f_{Q\ell}^{rs}$ in the numerator and of $|\mathcal{K}^{rs}|$, the total number of committed agents in the population (r, s) , to $Q q^{rs}$ in the denominator. This is a technical assumption to ensure that a revising agent can switch to paths not selected by any standard agents, thereby guaranteeing that the Markov chain has a unique stationary distribution. Payoffs are evaluated based on the population states of standard agents.

Let τ_n denote the random time at which the n -th revision opportunity occurs. The probability that an agent (r, s) taking path $k \in \mathcal{K}^{rs}$ receives a revision opportunity is f_{Qk}^{rs} ; thus, the transition probability of $\{F_Q^{\tau_n}\}_{n \in \mathbb{N}}$ is given by

$$\begin{aligned} \Pr \left[F_Q^{\tau_{n+1}} = \mathbf{f}_Q + \frac{1}{Q}(\mathbf{e}_\ell^{rs} - \mathbf{e}_k^{rs}) \mid F_Q^{\tau_n} = \mathbf{f}_Q \right] \\ = f_{Qk}^{rs} \frac{\rho_{k\ell}^{rs}(\mathbf{f}_Q) \exp[\eta^{-1} \pi_\ell^{rs}(\mathbf{f}_Q + \frac{1}{Q}(\mathbf{e}_\ell^{rs} - \mathbf{e}_k^{rs}))]}{\sum_{m \in \mathcal{K}^{rs}} \rho_{km}^{rs}(\mathbf{f}_Q) \exp[\eta^{-1} \pi_m^{rs}(\mathbf{f}_Q + \frac{1}{Q}(\mathbf{e}_m^{rs} - \mathbf{e}_k^{rs}))]}. \end{aligned} \quad (18)$$

According to Theorem 11.5.13 of Sandholm (2010), the stationary distribution of $\{F_Q^{\tau_n}\}$ is uniquely given by

$$\mu_Q(\mathbf{f}_Q) = \frac{1}{\kappa_Q} \exp[\eta^{-1} p_Q(\mathbf{f}_Q)], \quad (19)$$

for all $\mathbf{f}_Q \in \mathcal{F}_Q$, where κ_Q is determined so that $\sum_{\mathbf{f}_Q \in \mathcal{F}_Q} \mu_Q(\mathbf{f}_Q) = 1$, and μ_Q denotes the probability distribution over states; thus it can be used as a likelihood function.

However, a computational difficulty arises due to the normalizing constant κ_Q , because

⁵The stationary distribution of the Markov chain given by (19) remains unchanged across the entire class of *imitative exponential protocols*, including the imitative logit protocol.

the probabilities over all possible states should be computed. This is well recognized in the literature on the structural estimation of network games. Among others, Mele (2017) adopted the Bayesian approach, where an advanced version of the Metropolis-Hasting algorithm was used to bypass the computation of κ_Q .

In our context of road traffic assignment, the total number of agents can be considered large. We then consider the fact that $\frac{1}{Q} \ln \mu_Q$ is uniformly convergent in Q , and the limit function does not include the normalizing constant. Specifically, according to Theorem 12.2.7 of Sandholm (2010),

$$\lim_{Q \rightarrow \infty} \max_{\mathbf{f}_Q \in \mathcal{F}_Q} \left| \frac{1}{Q} \ln \mu_Q(\mathbf{f}_Q) - \frac{1}{\eta} \left\{ p(\mathbf{f}_Q) - \max_{\mathbf{f}' \in \mathcal{F}} p(\mathbf{f}') \right\} \right| = 0. \quad (20)$$

Therefore, under the supposition that Q is sufficiently large, the log likelihood $\ln \mu_Q(\mathbf{f}_Q)$ is proportional to $\eta^{-1} \{p(\mathbf{f}_Q) - \max_{\mathbf{f}' \in \mathcal{F}} p(\mathbf{f}')\}$, which replaces the task of computing the normalizing constant with the task of maximizing the potential function. In general, maximizing a function is not an easy task. However, as observed in Section 2, $p(\mathbf{f})$ depends on \mathbf{f} only through link flow rates \mathbf{y} : $p(\mathbf{f}) = g(\mathbf{y}(\mathbf{f}))$, where $g(\mathbf{y})$ is defined by (12), and g is strictly concave. In addition, by Lemma 2, the maximizer of g is the unique link flow induced by the Nash equilibrium of $\boldsymbol{\pi}$. Regarding the noise level $\eta > 0$, we normalize it to 1. Therefore, our log-likelihood function is given by

$$\ell(\theta|\mathbf{y}) = g(\mathbf{y}) - \max_{\mathbf{y}' \in \mathcal{Y}} g(\mathbf{y}'), \quad (21)$$

where $\mathcal{Y} = \{\mathbf{y} \in \mathbb{R}^{|\mathcal{L}|} : \exists \mathbf{f} \in \mathcal{F}, \mathbf{y} = \Delta \mathbf{f}\}$. Then we search for the maximum likelihood estimator $\hat{\theta} \in \arg \max_{\theta} \ell(\theta|\mathbf{y})$. Given the strict concavity of g , this is practically feasible.

3.2.2 Bootstrap method

To compute the standard errors for the estimator $\hat{\theta}$, we use a parametric bootstrap method. Specifically, for each $b = 0, 1, 2, \dots, B$, we generate a bootstrap dataset $\mathbf{f}_Q^b \sim \hat{\mu}_Q$, which follows the distribution in (19), with the potential function evaluated at $\hat{\theta}$. Next, We compute the estimate θ^b using the maximum likelihood method described in the previous subsection.

Sampling from $\hat{\mu}_Q$ presents computational challenges due to the normalizing constant, as previously noted. To address this issue, we use the Markov chain defined in (18), which is evaluated at $\hat{\theta}$. This Markov chain is constructed to have $\hat{\mu}_Q$ as its stationary distribution; thus, we generate population states according to (18), starting from an initial state $\mathbf{f}_Q^{(0)}$. As discussed in Sandholm (2010), the imitative logit protocol can be interpreted as a process of repeated sampling in which a revising agent randomly selects an opponent until deciding to adopt one of their paths. Therefore, the following steps are performed for $t = 0, 1, 2, \dots$ given $\mathbf{f}_Q^{(t)}$:

1. Draw a path according to the distribution $\mathbf{f}_Q^{(t)}$.
2. Suppose the selected path denoted by k belongs to the action set of the population (r, s) . Repeat the following steps until a new path is selected (cf. Izquierdo et al., 2019, Section 2.3):
 - (a) Randomly set an aspiration level $\gamma \in [0, \gamma_{\max}]$, where $\gamma_{\max} = \max_{m \in \mathcal{K}^{rs}} \exp[\pi_m^{rs}(\mathbf{f}_Q^{(t)})]$.
 - (b) Draw a candidate path $\ell \in \mathcal{K}^{rs}$ according to the distribution $\{\rho_{km}^{rs}(\mathbf{f}_Q^{(t)})\}_{m \in \mathcal{K}^{rs}}$.
 - (c) Switch to path ℓ if $\exp\left[\pi_\ell^{rs}\left(\mathbf{f}_Q^{(t)} + \frac{1}{Q}(\mathbf{e}_\ell^{rs} - \mathbf{e}_k^{rs})\right)\right] \geq \gamma$.
3. Let $\ell \in \mathcal{K}^{rs}$ be the path determined in the above step. Update the state as $\mathbf{f}_Q^{(t+1)} = \mathbf{f}_Q^{(t)} + \frac{1}{Q}(\mathbf{e}_\ell^{rs} - \mathbf{e}_k^{rs})$.

In general, a burn-in period is used to allow the Markov chain to approach its stationary distribution. To skip the burn-in period, we initialize the process by the equilibrium path flow rate \mathbf{f}_Q . However, as discussed in Section 2, the equilibrium path flow rate \mathbf{f}_Q is not generally unique. Rather than relying on the potential game approach, we use iTAPAS (Xie and Xie, 2016), a path-based algorithm for solving the user equilibrium (UE) assignment or the Nash equilibrium of the game $\boldsymbol{\pi}$. Among the potential multiple equilibria, the path flows obtained via iTAPAS are consistent with those that maximize the entropy $-\sum_{(r,s) \in \Omega} \sum_{k \in \mathcal{K}^{rs}} f_k^{rs} \ln[f_k^{rs}]$, which is commonly referred to as the "most likely path flows" (e.g., Bar-Gera, 2010; Xie and Xie, 2016).

To ensure sufficient switches, we treat the trajectories of the Markov chain as bootstrap samples every 500 periods.⁶ Specifically, we set $\mathbf{f}_Q^b = \mathbf{f}_Q^{(500b)}$ for $b = 0, 1, 2, \dots, B$, and use $B = 300$, which requires simulating the Markov chain for $500 \times 300 (= 150,000)$ periods.

3.3 Results

To solve the parameter estimation problem, we develop a hierarchical optimization algorithm that combines the conjugate direction Frank–Wolfe method (Mitradijeva and Lindberg, 2013) and Barzilai–Borwein method (Barzilai and Borwein, 1988). The developed algorithm allows us to rapidly and stably estimate the parameters. The details of the algorithm are presented in Appendix A. Using the developed algorithm, we perform the non-parametric bootstrap method. In other words, we solve the parameter estimation problems for 300 samples and obtain 300 parameters $(\alpha^{(1)}, \beta^{(1)}), \dots, (\alpha^{(300)}, \beta^{(300)})$.

Figures 3 and 4 show the estimated values of α and β for each sample. Table 1 summarizes the estimation results. The table shows the mean, standard deviation, maximum, and minimum values of the estimated parameters. The table also shows the quartiles and 0.25% and 97.5%

⁶Because the network in our data has 528 ODs, this approximately means that, on average, there is one switch in each population.

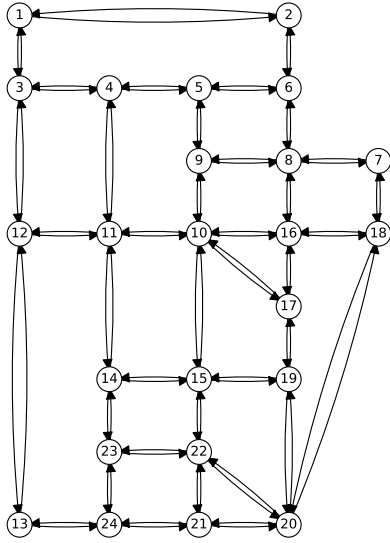


Figure 1: Sioux Falls network

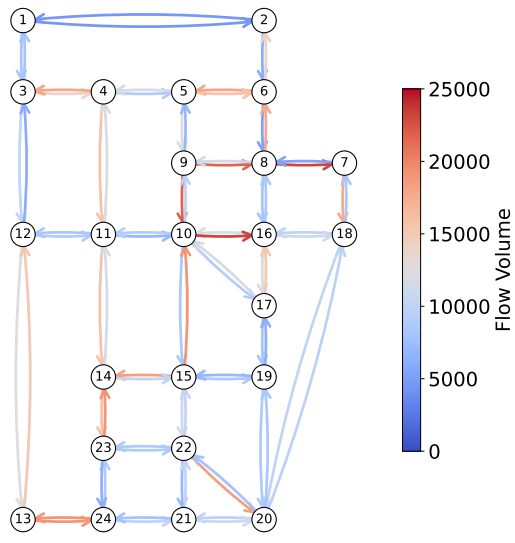


Figure 2: UE flow pattern

Table 1: Summary of the estimation results

	mean	std	min	2.5%	25.0%	50.0%	75.0%	97.5%	max
α	0.151	0.003	0.142	0.150	0.150	0.151	0.151	0.158	0.182
β	3.987	0.027	3.721	3.925	3.988	3.991	3.994	4.001	4.056

tile values. For all samples, the estimated parameters α and β are close to 0.15 and 4.0, respectively. In addition, the minimum and maximum values of the estimated results are not extreme outliers. Figures 5 and 6 illustrate the changes in the variance of the estimated parameters as the number of samples increases. For both α and β , the variance is nearly stable at 300 samples, even though there are slight variations up to 300 samples. These results imply that the non-parametric bootstrap method enables stable parameter estimation with almost 300 samples.

Figure 7 shows the joint distribution of the estimated values of α and β . The main area of the figure shows scatter plots of the estimated values for 300 samples, and the outside of the main area shows the surrounding distribution (histogram). The 95% confidence interval between the 0.25% and 97.5% tiles is indicated in gray, and the area where the α and β 95% confidence intervals overlap is expanded. The distributions of both the estimated values of α and β are unimodal.

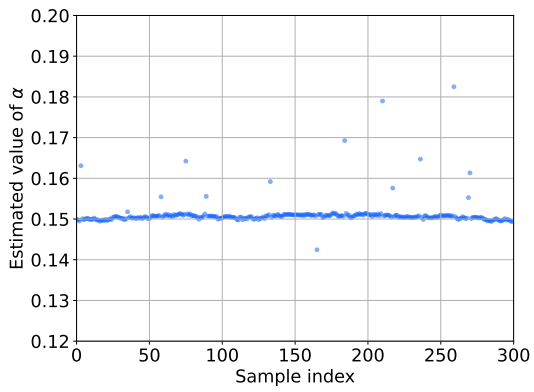


Figure 3: Estimated values of α for each sample

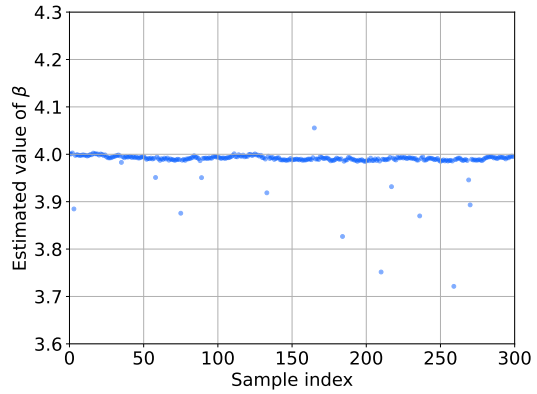


Figure 4: Estimated values of β for each sample

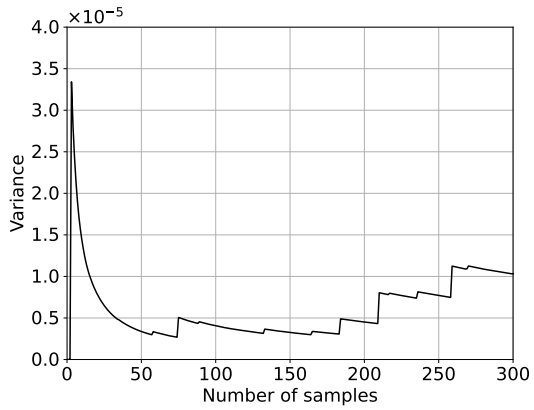


Figure 5: Variance of estimated value of α

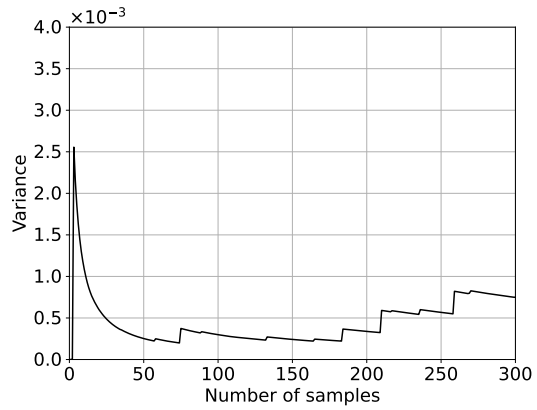


Figure 6: Variance of estimated value of β

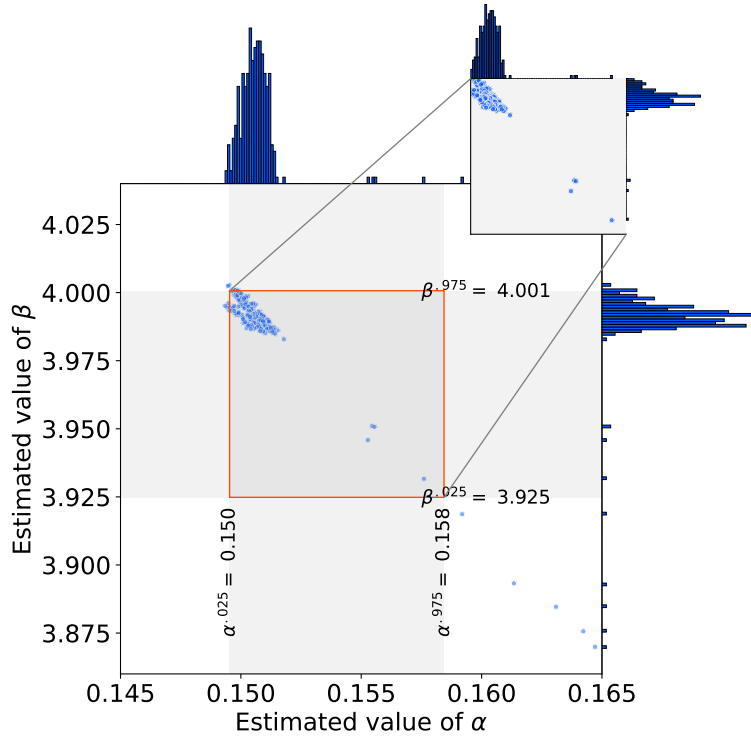


Figure 7: Joint distribution of the estimated values of α and β

4 Congestion pricing

The equilibrium of our model is generally inefficient due to negative externalities caused by congestion. To address this inefficiency, the planner aims to internalize these externalities by introducing congestion tolls, thereby reducing the social costs associated with traffic congestion. However, if the planner inaccurately estimates the external costs of congestion, congestion pricing may be unable to achieve an efficient allocation of agents.

This section evaluates the effectiveness of congestion tolls based on the estimated parameters discussed in Section 3, demonstrating the accuracy and practical applicability of our method. To this end, we first investigate the properties of the optimal congestion tolls in Section 4.1 and then analyze the effect of setting congestion tolls using estimated parameters, which may include errors, in Section 4.2. As discussed in the previous section, we assume that Q is sufficiently large; thus, our model can be considered a continuum-population game in this section.

4.1 Optimal congestion tolls

We define efficiency in terms of an aggregate payoff function $P(\mathbf{f})$, which can be defined as follows:

$$\begin{aligned} P(\mathbf{f}) &= \sum_{(r,s) \in \Omega} \sum_{k \in \mathcal{K}^{rs}} \pi_k^{rs}(\mathbf{f}) \cdot f_k^{rs} \\ &= - \sum_{(i,j) \in \mathcal{L}} t_{ij}(y_{ij}(\mathbf{f})) \cdot y_{ij}(\mathbf{f}). \end{aligned} \quad (22)$$

This expression shows that the total travel cost $\sum_{(i,j) \in \mathcal{L}} t_{ij}(y_{ij}(\mathbf{f})) \cdot y_{ij}(\mathbf{f})$ is minimized at the social optimum. Because the total travel cost is directly affected by the link flow rates $\mathbf{y}(\mathbf{f})$ rather than the population state \mathbf{f} , the aggregate payoff function can be equivalently redefined as $G(\mathbf{y}(\mathbf{f}))$, which is similar to the potential function.

$$G(\mathbf{y}) = - \sum_{(i,j) \in \mathcal{L}} t_{ij}(y_{ij}) \cdot y_{ij}(\mathbf{f}). \quad (23)$$

$t_{ij}(y_{ij})$ is a strictly increasing and convex function; thus, the Hessian matrix $\nabla^2 G(\mathbf{y})$ is negative definite, while $\nabla^2 P(\mathbf{f})$ is not. Thus, we obtain the following proposition.

Proposition 2 *The link flow rate $\mathbf{y}(\mathbf{f}^o) = (y_{ij}(\mathbf{f}^o))_{(i,j) \in \mathcal{L}}$ is uniquely determined at the social optimum, while the population state \mathbf{f}^o is generally non-unique.*

The optimal congestion toll c_k^{rs} for agent $(r, s) \in \Omega$ using path $k \in \mathcal{K}^{rs}$ is given by

$$\begin{aligned} c_k^{rs} &= \pi_k^{rs}(\mathbf{f}^o) - \frac{\partial G(\mathbf{y}(\mathbf{f}^o))}{\partial f_k^{rs}} \\ &= \sum_{(i,j) \in \mathcal{L}} t'_{ij}(y_{ij}(\mathbf{f}^o)) \cdot y_{ij}(\mathbf{f}^o) \cdot \delta_{ij,k}^{rs}, \end{aligned} \quad (24)$$

where $t'_{ij}(y_{ij}) = \frac{dt_{ij}(y_{ij})}{dy_{ij}}$. The above equation, along with Proposition 2, implies that the optimal toll levels depend only on the optimal link flow rates $\mathbf{y}(\mathbf{f}^o)$ and are uniquely determined. In addition, (24) reveals that c_k^{rs} is separable with respect to each link (i, j) . Therefore, the planner can internalize the congestion externalities by introducing the following tolls $\boldsymbol{\tau}^o = (\tau_{ij}^o)_{(i,j) \in \mathcal{L}}$ for the use of each link (i, j) :

$$\tau_{ij}^o = t'_{ij}(y_{ij}(\mathbf{f}^o)) \cdot y_{ij}(\mathbf{f}^o). \quad (25)$$

The optimal congestion toll $\boldsymbol{\tau}^o$ is effective for achieving the social optimum. To demonstrate this, we consider a situation in which the cost for traversing the link (i, j) is given by $t_{ij}(y_{ij}) + \tau_{ij}$, implying that the payoff $\hat{\pi}_k^{rs}(\mathbf{f} \mid \boldsymbol{\tau}^o)$ for agent (r, s) selecting path $k \in \mathcal{K}^{rs}$ is expressed as

follows:

$$\hat{\pi}_k^{rs}(\mathbf{f} \mid \boldsymbol{\tau}^o) = - \sum_{(i,j) \in \mathcal{L}} \{t_{ij}(y_{ij}(\mathbf{f})) + \tau_{ij}^o\} \delta_{ij,k}^{rs}. \quad (26)$$

Because $\boldsymbol{\tau}^o$ is independent of the population state \mathbf{f} , game $\hat{\pi}(\boldsymbol{\tau}^o)$ is a potential game with the following potential function $\hat{g}(\mathbf{y}(\mathbf{f}) \mid \boldsymbol{\tau}^o)$:

$$\hat{g}(\mathbf{y}(\mathbf{f}) \mid \boldsymbol{\tau}^o) = g(\mathbf{y}(\mathbf{f})) + \sum_{(i,j) \in \mathcal{L}} \tau_{ij}^o y_{ij}(\mathbf{f}). \quad (27)$$

Because $\boldsymbol{\tau}^o$ is given by (25), the optimal population state \mathbf{f}^o satisfies the KKT conditions for the maximization problem $\max_{\mathbf{f} \in \mathcal{F}} \hat{g}(\mathbf{y}(\mathbf{f}) \mid \boldsymbol{\tau}^o)$, implying that \mathbf{f}^o is an equilibrium of game $\hat{\pi}$. $\nabla^2 \hat{g}(\mathbf{y} \mid \boldsymbol{\tau}^o) = \nabla^2 g(\mathbf{y})$ is negative definite, whereas $\nabla^2 \hat{g}(\mathbf{y}(\mathbf{f}) \mid \boldsymbol{\tau}^o)$ is not. Therefore, we obtain the following proposition.

Proposition 3 *In the continuum-population game $\hat{\pi}(\boldsymbol{\tau}^o)$, the equilibrium population state $\hat{\mathbf{f}}^*$ is generally non-unique. However, the equilibrium link flow rates $\mathbf{y}(\hat{\mathbf{f}}^*)$ are uniquely determined and are equivalent to $\mathbf{y}(\mathbf{f}^o)$.*

This result indicates that the planner can achieve optimal allocation by introducing the optimal congestion tolls $\boldsymbol{\tau}^o$.

Directly computing the optimal link flow rate $\mathbf{y}(\mathbf{f}^o)$ or $\mathbf{y}(\hat{\mathbf{f}}^*)$ is infeasible, because defining \mathbf{f} requires enumerating all possible paths in the network. In Section 2, we addressed this challenge in the potential maximization problem by reformulating it in terms of link flow rates by each origin rather than individual paths. Similarly, we reformulate the problem of maximizing $G(\mathbf{y}(\mathbf{f}))$ or $\hat{g}(\mathbf{y}(\mathbf{f}) \mid \boldsymbol{\tau}^o)$ to avoid explicit path enumeration. The reformulation results in the following link-based optimization problems:

$$\max_{\mathbf{x} \in \mathbb{R}_+^{|\mathcal{L}| \times |\mathcal{R}|}} G(\hat{\mathbf{y}}(\mathbf{x})) \quad \text{s.t. (13b)}, \quad (28a)$$

$$\max_{\mathbf{x} \in \mathbb{R}_+^{|\mathcal{L}| \times |\mathcal{R}|}} \hat{g}(\hat{\mathbf{y}}(\mathbf{x}) \mid \boldsymbol{\tau}^o) \quad \text{s.t. (13b)}. \quad (28b)$$

This approach enables efficient computation of the optimal link flow rate $\hat{\mathbf{y}}(\mathbf{x}^o)$, which is equivalent to $\mathbf{y}(\mathbf{f}^o)$ and $\mathbf{y}(\hat{\mathbf{f}}^*)$, thereby facilitating the analysis and application of congestion tolls in large networks.

4.2 Effects of congestion tolls based on estimated parameters

When setting optimal congestion tolls, the planner needs precise values of the link cost function parameters, because these values determine the external costs of congestion. However, evaluating the accuracy of the estimates of these parameters can be challenging, even if the

precise values are known. Even a small estimation error may yield congestion tolls that fail to improve the total travel cost. Because of this sensitivity, improvements in the total travel costs due to congestion tolls are a practical measure of the accuracy of the parameter estimates: if the estimated values are sufficiently precise, we expect substantial improvements, indicating that the congestion tolls are near-optimal.

In this analysis, we use 300 bootstrap samples of the estimated parameters obtained in Section 3 to calculate the distribution of the total travel cost improvements. This distribution reflects the robustness of the parameter estimates and provides insights into the practicability of congestion tolls set using these values.

We assume that for each bootstrap sample, the planner sets the congestion toll $\boldsymbol{\tau}(\theta^{(n)})$ using the estimated parameters $\theta^{(n)} = (\alpha^{(n)}, \beta^{(n)})$, whereas the true parameter values are $\theta^* = (0.15, 4.0)$. Specifically, the planner solves the problem (28) using the parameters $\theta^{(n)}$ to obtain the optimal link flow rate $\hat{\boldsymbol{y}}(\boldsymbol{x}^o(\theta^{(n)}))$ and then sets

$$\tau_{ij}(\theta^{(n)}) = \bar{t}_{ij} \alpha^{(n)} \beta^{(n)} \left(\frac{\hat{y}_{ij}(\boldsymbol{x}^o(\theta^{(n)}))}{\mu_{ij}} \right)^{\beta^{(n)}}. \quad (29)$$

Because agents select their paths to minimize travel costs under the parameters θ^* , the actual optimal congestion toll is $\boldsymbol{\tau}^o = \boldsymbol{\tau}(\theta^*)$ but not $\boldsymbol{\tau}(\theta^{(n)})$, implying that the planner cannot achieve the social optimum.

With this setup, we evaluate changes in the total travel cost resulting from introducing the non-optimal congestion toll $\boldsymbol{\tau}(\theta^{(n)})$. Let $\hat{\boldsymbol{y}}(\boldsymbol{x}^*(\boldsymbol{\tau}(\theta^{(n)})))$ denote the equilibrium link flow rate of game $\hat{\boldsymbol{\pi}}(\boldsymbol{\tau}(\theta^{(n)}))$ under the true parameters θ^* . This link flow rate is calculated by solving the maximization problem (28b) and replacing the potential function with $\hat{g}(\boldsymbol{x} \mid \boldsymbol{\tau}(\theta^{(n)}))$. The total travel cost $T(\boldsymbol{\tau}(\theta^{(n)}))$ at the equilibrium of game $\hat{\boldsymbol{\pi}}(\boldsymbol{\tau}(\theta^{(n)}))$ is given by

$$T(\boldsymbol{\tau}(\theta^{(n)})) = \sum_{(i,j) \in \mathcal{L}} t_{ij}(\hat{y}_{ij}(\boldsymbol{x}^*(\theta^{(n)}))) \cdot \hat{y}_{ij}(\boldsymbol{x}^*(\theta^{(n)})) \quad (30)$$

The equilibrium link flow rate without congestion tolls corresponds to $\hat{\boldsymbol{y}}(\boldsymbol{x}^*(\mathbf{0}))$; thus, the improvement in the total travel cost resulting from introducing the congestion toll $\boldsymbol{\tau}(\theta^{(n)})$ for the (n) -th bootstrap sample is given by

$$R^{(n)} = \frac{T(\boldsymbol{\tau}(\theta^{(n)})) - T(\mathbf{0})}{T(\mathbf{0})} \times 100, \quad (31)$$

where $R^{(n)}$ denotes the rate of change in the total travel cost caused by introducing the congestion toll $\boldsymbol{\tau}(\theta^{(n)})$. We also define the rate of change in the total travel cost when the congestion toll $\boldsymbol{\tau}(\theta^*)$, based on the exact parameter, is implemented as follows:

$$R^* = \frac{T(\boldsymbol{\tau}(\theta^*)) - T(\mathbf{0})}{T(\mathbf{0})} \times 100. \quad (32)$$

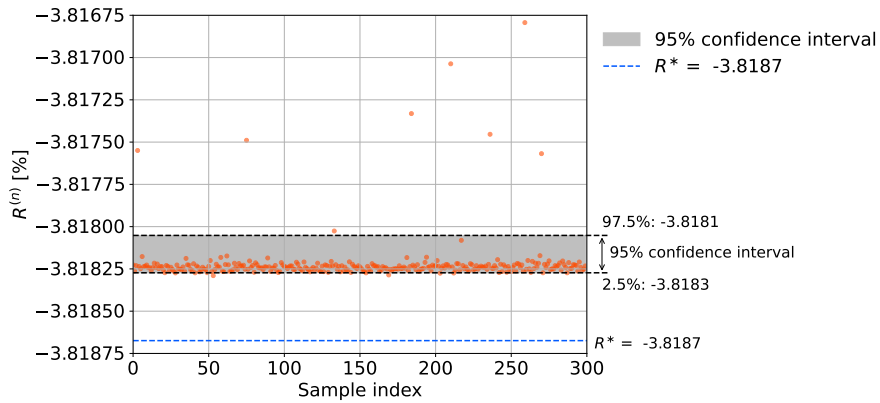


Figure 8: Efficiency of congestion tolls based on estimated parameters

Figure 8 shows a scatter plot illustrating the distribution of improvements in the total travel cost ($R^{(n)}$ values) across all bootstrap samples and R^* , with 0.25% and 97.5% tiles indicated by dashed lines. The result shows that across all samples, the tolls based on the estimated parameters reduce the total travel cost by approximately 3.8%. This result indicates that congestion tolls based on estimated parameters improve efficiency nearly as much as those based on the exact parameters.

5 Conclusion

This paper presented a structural estimation approach for evaluating congestion externalities in transportation networks by modeling travelers' route choices as a stochastic evolutionary game. We demonstrated the effectiveness of the proposed estimation method by accurately identifying the parameters of the BPR function from the simulated traffic data. Using bootstrap sampling, we confirmed the robustness and consistency of the estimated values across various samples. The proposed approach accounts for the complexities of route choices and congestion impacts on travel costs, providing a robust method for estimating the parameters of the link cost function.

In addition, this paper evaluated the impact of setting congestion tolls based on these estimated parameters, including the sensitivity of the total travel cost improvements to estimation accuracy. Our results reveal that even with estimation errors, congestion tolling based on the proposed approach significantly reduces the total travel cost across all bootstrap samples. This result highlights the resilience of the proposed method to estimation deviations, demonstrating its practical viability for improving network efficiency even with imperfect parameter precision.

These results contribute to an accurate and practical estimation method that can improve the efficiency of congestion pricing strategies. Demonstrated in a simulated environment, the proposed approach represents a first step toward future studies using real-world traffic data, such as data from fixed traffic detectors and probe vehicles. As a next step, applying the proposed model to actual road networks will enable its validation under varied, real-world conditions and provide insights into optimizing congestion tolls on a larger scale.

A Algorithm

A.1 Hierarchical algorithm

This section presents a hierarchical algorithm for solving the parameter estimation problem that maximizes log-likelihood function (21). The algorithm integrates the conjugate direction Frank–Wolfe method (Mitradjieva and Lindberg, 2013) and Barzilai–Borwein method (Barzilai and Borwein, 1988). By combining these two methods hierarchically, the algorithm achieves both efficiency and accuracy.

The estimation problem is written as follows:

$$\max_{\boldsymbol{\theta} \in \mathbb{R}_+^2} \ell(\boldsymbol{\theta} \mid \mathbf{y}) = g(\mathbf{y} \mid \boldsymbol{\theta}) - \max_{\mathbf{y}' \in \mathcal{Y}} g(\mathbf{y}' \mid \boldsymbol{\theta}). \quad (33)$$

We decompose the problem into the master and sub-problems as follows:

$$\text{[Master]} \quad \max_{\boldsymbol{\theta} \in \mathbb{R}_+^2} \ell(\boldsymbol{\theta} \mid \mathbf{y}) = g(\mathbf{y} \mid \boldsymbol{\theta}) - g^*(\boldsymbol{\theta}) \quad (34)$$

$$\text{[Sub]} \quad g^*(\boldsymbol{\theta}) \equiv \max_{\mathbf{y}' \in \mathcal{Y}} g(\mathbf{y}' \mid \boldsymbol{\theta}) \quad (35)$$

where $g^*(\boldsymbol{\theta})$ denotes the optimal value function of the sub-problem. The sub-problem [Sub] is a standard UE assignment and is a convex optimization problem. In contrast, the master problem [Master] is a non-negative constrained optimization problem. We apply the conjugate direction Frank–Wolfe method for the sub-problem [Sub] and the Barzilai–Borwein method for the master problem [Master].⁷

The conjugate direction Frank–Wolfe method for the UE problem is proposed by Mitradjieva and Lindberg (2013). This algorithm uses the classical Frank–Wolfe and conjugate directions to update the variables. By combining the two directions, the algorithm can avoid a part of the zigzag phenomenon around the final solution.

The Barzilai–Borwein method is designed for unconstrained optimization. This method is an iterative gradient descent method that uses the step sizes derived from the linear trend of the most recent two iterates. The algorithm is shown in Algorithm 1. At step 2 in Algorithm 1, the gradient $\nabla \ell(\boldsymbol{\theta} \mid \mathbf{y})$ can be calculated in the following processes. Based on the envelope theorem, we obtain the gradient of the optimal value function of the sub-problem as follows:

$$\frac{\partial g^*(\boldsymbol{\theta})}{\partial \alpha} = - \sum_{(i,j) \in \mathcal{L}} \bar{t}_{ij} \frac{1}{\beta + 1} y_{ij}^* \left(\frac{y_{ij}^*}{\tilde{\mu}_{ij}} \right)^\beta, \quad (36)$$

⁷Both methods were originally designed for minimization problems. We adapt these methods to our maximization problem by reversing the sign of the objective function and converting the maximization problem into a minimization problem.

Algorithm 1 Barzilai–Borwein method

Input: $\boldsymbol{\theta}^{(0)} \in \mathbb{R}_+^2$

- 1: **for** $k = 1, 2, \dots$ **do**
- 2: Compute $\nabla \ell(\boldsymbol{\theta}^{(k)} \mid \mathbf{y})$ by solving the sub-problem
- 3: Compute $a^{(k)}$ by Eq.(41)
- 4: $\boldsymbol{\theta}^{(k+1)} \leftarrow \max \{ \mathbf{0}, \boldsymbol{\theta}^{(k)} + a^{(k)} \nabla \ell(\boldsymbol{\theta}^{(k)} \mid \mathbf{y}) \}$
- 5: Check the stop criterion
- 6: **end for**

Output: $\boldsymbol{\theta}^{(k)}$

$$\frac{\partial g^*(\boldsymbol{\theta})}{\partial \beta} = - \sum_{(i,j) \in \mathcal{L}} \bar{t}_{ij} \alpha y_{ij}^* \left[\frac{1}{\beta + 1} \left(\frac{y_{ij}^*}{\tilde{\mu}_{ij}} \right)^\beta \ln \left(\frac{y_{ij}^*}{\tilde{\mu}_{ij}} \right) - \frac{1}{(\beta + 1)^2} \left(\frac{y_{ij}^*}{\tilde{\mu}_{ij}} \right)^\beta \right] \quad (37)$$

$$= - \sum_{(i,j) \in \mathcal{L}} \bar{t}_{ij} \alpha y_{ij}^* \frac{1}{\beta + 1} \left(\frac{y_{ij}^*}{\tilde{\mu}_{ij}} \right)^\beta \left[\ln \left(\frac{y_{ij}^*}{\tilde{\mu}_{ij}} \right) - \frac{1}{\beta + 1} \right], \quad (38)$$

where $\tilde{\mu}_{ij}$ denotes the relative capacity, i.e., $\tilde{\mu}_{ij} \equiv \mu_{ij}/Q$. Using $\nabla p^*(\boldsymbol{\theta})$, we obtain

$$\frac{\partial \ell(\boldsymbol{\theta} \mid \mathbf{y})}{\partial \alpha} = - \sum_{(i,j) \in \mathcal{L}} \bar{t}_{ij} \frac{1}{\beta + 1} y_{ij} \left(\frac{y_{ij}}{\tilde{\mu}_{ij}} \right)^\beta + \sum_{(i,j) \in \mathcal{L}} \bar{t}_{ij} \frac{1}{\beta + 1} y_{ij}^* \left(\frac{y_{ij}^*}{\tilde{\mu}_{ij}} \right)^\beta \quad (39)$$

$$\begin{aligned} \frac{\partial \ell(\boldsymbol{\theta} \mid \mathbf{y})}{\partial \beta} = & - \sum_{(i,j) \in \mathcal{L}} \bar{t}_{ij} \alpha y_{ij} \frac{1}{\beta + 1} \left(\frac{y_{ij}}{\tilde{\mu}_{ij}} \right)^\beta \left[\ln \left(\frac{y_{ij}}{\tilde{\mu}_{ij}} \right) - \frac{1}{\beta + 1} \right] \\ & + \sum_{(i,j) \in \mathcal{L}} \bar{t}_{ij} \alpha y_{ij}^* \frac{1}{\beta + 1} \left(\frac{y_{ij}^*}{\tilde{\mu}_{ij}} \right)^\beta \left[\ln \left(\frac{y_{ij}^*}{\tilde{\mu}_{ij}} \right) - \frac{1}{\beta + 1} \right]. \end{aligned} \quad (40)$$

The step size $a^{(k)}$, at step 3 in Algorithm 1, is determined as follows:

$$a^{(k)} = \frac{[\boldsymbol{\theta}^{(k)} - \boldsymbol{\theta}^{(k-1)}]^\top [\nabla \ell(\boldsymbol{\theta}^{(k)}) - \nabla \ell(\boldsymbol{\theta}^{(k-1)})]}{[\nabla \ell(\boldsymbol{\theta}^{(k)}) - \nabla \ell(\boldsymbol{\theta}^{(k-1)})]^\top [\nabla \ell(\boldsymbol{\theta}^{(k)}) - \nabla \ell(\boldsymbol{\theta}^{(k-1)})]} \quad \forall k = 2, 3, \dots \quad (41)$$

At step 4 in Algorithm 1, the variables are updated using the step size. In this step, the projection onto the nonnegative area is performed simultaneously.

A.2 Numerical example

This section presents a numerical example to demonstrate the efficiency and accuracy of the algorithm. Specifically, we demonstrate the parameter estimation results when the observation flow pattern is the UE flow pattern, as calculated using iTAPAS in Section 3.2. Because the observation flow is the UE flow, the actual parameter values (i.e., $\alpha^* = 0.15$ and $\beta^* = 4.0$) are

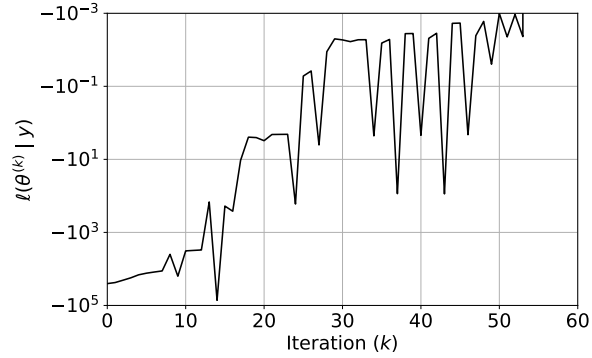


Figure 9: $\ell(\boldsymbol{\theta}^{(k)} | \mathbf{y})$ during iteration

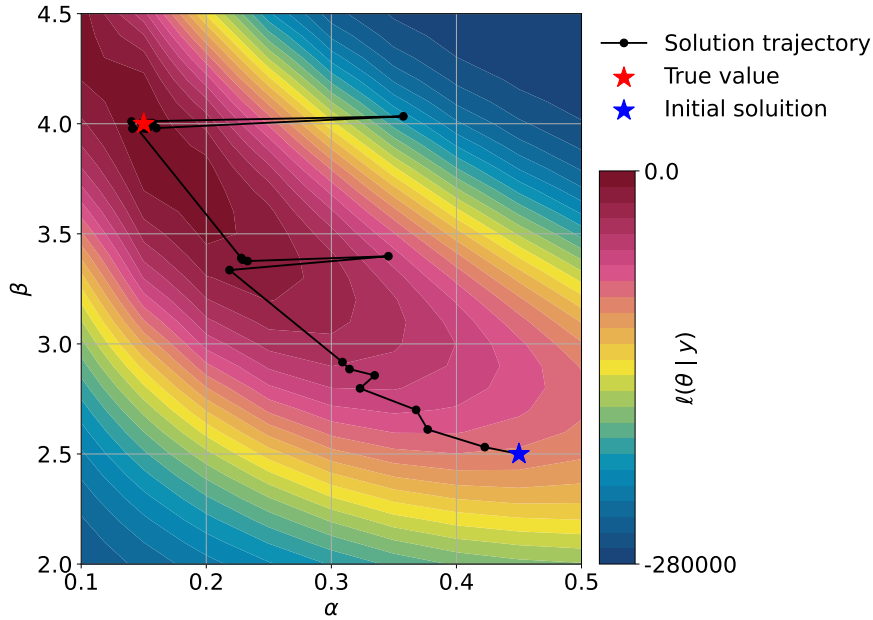


Figure 10: Solution trajectory during iteration

expected to be estimated.

We solve the parameter estimation problem based on the above settings using the hierarchical algorithm. Consequently, we obtain the estimated values $\hat{\alpha} = 0.1498$ and $\hat{\beta} = 4.0010$. The number of iterations of the Barzilai–Borwein method for the master problem is 54, and the calculation wall time is 11.3 [s]. Figure 9 illustrates the value of $\ell(\boldsymbol{\theta}^{(k)} | \mathbf{y})$ during the iteration of the Barzilai–Borwein method for the master problem. The value of $\ell(\boldsymbol{\theta}^{(k)} | \mathbf{y})$ increases with some oscillation. Figure 10 shows the solution trajectory during the algorithm iteration. In the figure, the contour lines of $\ell(\boldsymbol{\theta} | \mathbf{y})$ are colored. The blue and red stars represent the initial solution (i.e., $\alpha^{(0)} = 0.45$, $\beta^{(0)} = 2.5$) and the true value of the parameter (i.e., $\alpha^* = 0.15$, $\beta^* = 4.0$), respectively. These results demonstrate that the proposed method is fast and accurate in parameter estimation.

B Data details

Tables 2, 3, and 4 show detailed information about the Sioux Falls network data provided by Transportation Networks for Research Core Team.

C Proofs

C.1 Proof of Lemma 1

Because $\int_0^{y_{ij}(\mathbf{f}_Q)} t_{ij}(z) dz = \sum_{v=1}^{Q y_{ij}(\mathbf{f}_Q)} \int_{v-1}^v t_{ij}\left(\frac{z}{Q}\right) dz$ and $\frac{1}{Q} t_{ij}\left(\frac{v}{Q}\right) = \int_{\frac{v-1}{Q}}^{\frac{v}{Q}} t_{ij}\left(\frac{v}{Q}\right) dz$,

$$\sum_{v=1}^{Q y_{ij}(\mathbf{f}_Q)} t_{ij}\left(\frac{v}{Q}\right) \frac{1}{Q} - \int_0^{y_{ij}(\mathbf{f}_Q)} t_{ij}(z) dz = \sum_{v=1}^{Q y_{ij}(\mathbf{f}_Q)} \int_{\frac{v-1}{Q}}^{\frac{v}{Q}} \left[t_{ij}\left(\frac{v}{Q}\right) - t_{ij}(z) \right] dz \quad (42)$$

By the mean value theorem, there exists $c_v \in [z, \frac{v}{Q}]$ such that $t_{ij}\left(\frac{v}{Q}\right) - t_{ij}(z) = (\frac{v}{Q} - z) t'_{ij}(c_v)$. Therefore,

$$\begin{aligned} \left| \sum_{v=1}^{Q y_{ij}(\mathbf{f}_Q)} t_{ij}\left(\frac{v}{Q}\right) \frac{1}{Q} - \int_0^{y_{ij}(\mathbf{f}_Q)} t_{ij}(z) dz \right| &\leq \sum_{v=1}^{Q y_{ij}(\mathbf{f}_Q)} \left| t'_{ij}(c_v) \int_{\frac{v-1}{Q}}^{\frac{v}{Q}} \left(\frac{v}{Q} - z\right) dz \right| \\ &= \sum_{v=1}^{Q y_{ij}(\mathbf{f}_Q)} |t'_{ij}(c_v)| \frac{1}{2Q^2} \\ &\leq \frac{y_{ij}(\mathbf{f}_Q)}{2Q} \max_{x \in [0, y_{ij}(\mathbf{f}_Q)]} |t'_{ij}(x)| \rightarrow 0 \text{ as } Q \rightarrow \infty. \end{aligned} \quad (43)$$

□

C.2 Proof of Proposition 1

Let $\hat{p}(\mathbf{y})$ be a function of \mathbf{y} corresponding to the potential function (9):

$$\hat{p}(\mathbf{y}) = - \sum_{(i,j) \in \mathcal{L}} \int_0^{y_{ij}} t_{ij}(z) dz. \quad (44)$$

\hat{p} is strictly concave because the Hessian matrix of \hat{p} is negative definite.

$$\frac{\partial^2 \hat{p}(\mathbf{y})}{\partial y_{ij} \partial y_{\hat{i}\hat{j}}} = \begin{cases} -\frac{dt_{ij}(y_{ij})}{dy_{ij}} < 0 & \text{if } (i, j) = (\hat{i}, \hat{j}), \\ 0 & \text{otherwise.} \end{cases} \quad (45)$$

This implies that the link flow rate \mathbf{y}^* that maximizes the potential function (9) is uniquely determined. The uniqueness of the link flow rate \mathbf{y}^* implies that all link costs $\mathbf{t} = (t_{ij}(y_{ij}))_{(i,j) \in \mathcal{L}}$

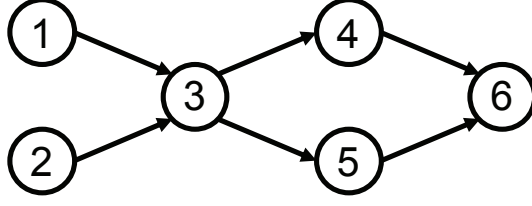


Figure 11: simple network

and the travel costs C are also uniquely determined at the equilibrium.

However, the equilibrium state \mathbf{f}^* is generally non-unique, as demonstrated in Sheffi (1985). This non-uniqueness occurs because multiple path flow rates can produce the same link flow rate \mathbf{y} . This is illustrated using a simple network with $\Omega = \{(1, 6), (2, 6)\}$ in Figure 11. If the link flow pattern is given by

$$y_{12} = q_{16}, \quad y_{13} = q_{26}, \quad y_{34} = y_{46} = Y_1 < q_{16} + q_{26}, \quad y_{35} = y_{56} = q_{16} + q_{26} - Y_1, \quad (46)$$

this link flow pattern can be achieved by any path flow pattern \mathbf{f} that satisfies

$$f_k^{16} = \begin{cases} \psi & \text{for the path } 1 \rightarrow 3 \rightarrow 4 \rightarrow 6, \\ q_{16} - \psi & \text{for the path } 1 \rightarrow 3 \rightarrow 5 \rightarrow 6, \end{cases} \quad (47a)$$

$$f_k^{26} = \begin{cases} Y_1 - \psi & \text{for the path } 2 \rightarrow 3 \rightarrow 4 \rightarrow 6, \\ q_{26} - Y_1 + \psi & \text{for the path } 2 \rightarrow 3 \rightarrow 5 \rightarrow 6, \end{cases} \quad (47b)$$

with $\psi \in [\max\{0, Y_1 - q_{26}\}, \min\{Y_1, q_{16}\}]$. □

References

- AKAMATSU, T. (1997): “Decomposition of Path Choice Entropy in General Transport Networks,” *Transportation Science*, 31, 349–362.
- ALLEN, T. AND C. ARKOLAKIS (2022): “The Welfare Effects of Transportation Infrastructure Improvements,” *The Review of Economic Studies*, 89, 2911–2957.
- ALMAGRO, M., F. BARBIERI, J. C. CASTILLO, N. G. HICKOK, AND T. SALZ (2024): “Optimal Urban Transportation Policy: Evidence from Chicago,” *NBER WORKING PAPER SERIES*.
- BAR-GERA, H. (2010): “Traffic Assignment by Paired Alternative Segments,” *Transportation Research Part B: Methodological*, 44, 1022–1046.
- BARZILAI, J. AND J. M. BORWEIN (1988): “Two-point step size gradient methods,” *IMA journal of numerical analysis*, 8, 141–148.
- DURMEYER, I. AND N. MARTINEZ (2022): “The welfare consequences of urban traffic regulations,” .
- FAJGELBAUM, P. D. AND E. SCHAAL (2020): “Optimal Transport Networks in Spatial Equilibrium,” *Econometrica*, 88, 1411–1452.
- HSIEH, C.-S., M. D. KÖNIG, AND X. LIU (2022): “A Structural Model for the Coevolution of Networks and Behavior,” *The Review of Economics and Statistics*, 104, 355–367.
- IZQUIERDO, L. R., S. S. IZQUIERDO, AND W. H. SANDHOLM (2019): *Agent-Based Evolutionary Game Dynamics*, Independent.
- MELE, A. (2017): “A Structural Model of Dense Network Formation,” *Econometrica*, 85, 825–850.
- MITRADJIEVA, M. AND P. O. LINDBERG (2013): “The stiff is moving—conjugate direction Frank-Wolfe methods with applications to traffic assignment,” *Transportation science*, 47, 280–293.
- MONDERER, D. AND L. S. SHAPLEY (1996): “Potential Games,” *Games and Economic Behavior*, 14, 124–143.
- NAKAJIMA, R. (2007): “Measuring Peer Effects on Youth Smoking Behaviour,” *The Review of Economic Studies*, 74, 897–935.
- ROSENTHAL, R. W. (1973): “A Class of Games Possessing Pure-Strategy Nash Equilibria,” *International Journal of Game Theory*, 2, 65–67.

- SANDHOLM, W. H. (2001): “Potential Games with Continuous Player Sets,” *Journal of Economic Theory*, 97, 81–108.
- (2010): *Population Games and Evolutionary Dynamics*, MIT Press.
- (2015): “Population Games and Deterministic Evolutionary Dynamics,” in *Handbook of Game Theory*, ed. by H. P. Young and S. Zamir, Elsevier B.V., vol. 4, 703–778.
- SHEFFI, Y. (1985): *Urban transportation networks: Equilibrium analysis with mathematical programming methods*, Harlow, England: Longman Higher Education.
- SMALL, K. A., E. T. VERHOEF, AND R. LINDSEY (2024): *The Economics of Urban Transportation*, Routledge, third ed.
- TRANSPORTATION NETWORKS FOR RESEARCH CORE TEAM (Accessed: September 22, 2024): “Transportation Networks for Research,” <https://github.com/bstabler/TransportationNetworks>.
- U.S. BUREAU OF PUBLIC ROADS (1964): *Traffic Assignment Manual*, U.S. Department of Commerce, Washington, D.C.
- VIAUROUX, C. (2011): “Pricing Urban Congestion: A Structural Random Utility Model with Traffic Anticipation,” *European Economic Review*, 55, 877–902.
- XIE, J. AND C. XIE (2016): “New insights and improvements of using paired alternative segments for traffic assignment,” *Transportation Research Part B: Methodological*, 93, 406–424.

Table 2: Link information

link id	start	end	capacity μ_{ij}	fft \bar{t}_{ij}	link id	start	end	capacity μ_{ij}	fft \bar{t}_{ij}
0	1	2	25900.200	6	38	13	24	5091.256	4
1	1	3	23403.470	4	39	14	11	4876.508	4
2	2	1	25900.200	6	40	14	15	5127.526	5
3	2	6	4958.181	5	41	14	23	4924.791	4
4	3	1	23403.470	4	42	15	10	13512.000	6
5	3	4	17110.520	4	43	15	14	5127.526	5
6	3	12	23403.470	4	44	15	19	14564.75	3
7	4	3	17110.520	4	45	15	22	9599.181	3
8	4	5	17782.790	2	46	16	8	5045.823	5
9	4	11	4908.827	6	47	16	10	4854.918	4
10	5	4	17782.790	2	48	16	17	5229.910	2
11	5	6	4947.995	4	49	16	18	19679.900	3
12	5	9	10000.000	5	50	17	10	4993.511	8
13	6	2	4958.181	5	51	17	16	5229.910	2
14	6	5	4947.995	4	52	17	19	4823.951	2
15	6	8	4898.588	2	53	18	7	23403.470	2
16	7	8	7841.811	3	54	18	16	19679.900	3
17	7	18	23403.470	2	55	18	20	23403.470	4
18	8	6	4898.588	2	56	19	15	14564.750	3
19	8	7	7841.811	3	57	19	17	4823.951	2
20	8	9	5050.193	10	58	19	20	5002.608	4
21	8	16	5045.823	5	59	20	18	23403.470	4
22	9	5	10000.000	5	60	20	19	5002.608	4
23	9	8	5050.193	10	61	20	21	5059.912	6
24	9	10	13915.790	3	62	20	22	5075.697	5
25	10	9	13915.790	3	63	21	20	5059.912	6
26	10	11	10000.000	5	64	21	22	5229.910	2
27	10	15	13512.000	6	65	21	24	4885.358	3
28	10	16	4854.918	4	66	22	15	9599.181	3
29	10	17	4993.511	8	67	22	20	5075.697	5
30	11	4	4908.827	6	68	22	21	5229.910	2
31	11	10	10000.000	5	69	22	23	5000.000	4
32	11	12	4908.827	6	70	23	14	4924.791	4
33	11	14	4876.508	4	71	23	22	5000.000	4
34	12	3	23403.470	4	72	23	24	5078.508	2
35	12	11	4908.827	6	73	24	13	5091.256	4
36	12	13	25900.200	3	74	24	21	4885.358	3
37	13	12	25900.200	3	75	24	23	5078.508	2

Table 3: OD demand $\{Q^{rs}\}$ in SiouxFalls network (1-12)

O / D	1	2	3	4	5	6	7	8	9	10	11	12
1	0	100	100	500	200	300	500	800	500	1300	500	200
2	100	0	100	200	100	400	200	400	200	600	200	100
3	100	100	0	200	100	300	100	200	100	300	300	200
4	500	200	200	0	500	400	400	700	700	1200	1400	600
5	200	100	100	500	0	200	200	500	800	1000	500	200
6	300	400	300	400	200	0	400	800	400	800	400	200
7	500	200	100	400	200	400	0	1000	600	1900	500	700
8	800	400	200	700	500	800	1000	0	800	1600	800	600
9	500	200	100	700	800	400	600	800	0	2800	1400	600
10	1300	600	300	1200	1000	800	1900	1600	2800	0	4000	2000
11	500	200	300	1500	500	400	500	800	1400	3900	0	1400
12	200	100	200	600	200	200	700	600	600	2000	1400	0
13	500	300	100	600	200	200	400	600	600	1900	1000	1300
14	300	100	100	500	100	100	200	400	600	2100	1600	700
15	500	100	100	500	200	200	500	600	1000	4000	1400	700
16	500	400	200	800	500	900	1400	2200	1400	4400	1400	700
17	400	200	100	500	200	500	1000	1400	900	3900	1000	600
18	100	0	0	100	0	100	200	300	200	700	200	200
19	300	100	0	200	100	200	400	700	400	1800	400	300
20	300	100	0	300	100	300	500	900	600	2500	600	500
21	100	0	0	200	100	100	200	400	300	1200	400	300
22	400	100	100	400	200	200	500	500	700	2600	1100	700
23	300	0	100	500	100	100	200	300	500	1800	1300	700
24	100	0	0	200	0	100	100	200	200	800	600	500

Table 4: OD demand $\{Q^{rs}\}$ in SiouxFalls network (13-24)

O / D	13	14	15	16	17	18	19	20	21	22	23	24
1	500	300	500	500	400	100	300	300	100	400	300	100
2	300	100	100	400	200	0	100	100	0	100	0	0
3	100	100	100	200	100	0	0	0	0	100	100	0
4	600	500	500	800	500	100	200	300	200	400	500	200
5	200	100	200	500	200	0	100	100	100	200	100	0
6	200	100	200	900	500	100	200	300	100	200	100	100
7	400	200	500	1400	1000	200	400	500	200	500	200	100
8	600	400	600	2200	1400	300	700	900	400	500	300	200
9	600	600	900	1400	900	200	400	600	300	700	500	200
10	1900	2100	4000	4400	3900	700	1800	2500	1200	2600	1800	800
11	1000	1600	1400	1400	1000	100	400	600	400	1100	1300	600
12	1300	700	700	700	600	200	300	400	300	700	700	500
13	0	600	700	600	500	100	300	600	600	1300	800	800
14	600	0	1300	700	700	100	300	500	400	1200	1100	400
15	700	1300	0	1200	1500	200	800	1100	800	2600	1000	400
16	600	700	1200	0	2800	500	1300	1600	600	1200	500	300
17	500	700	1500	2800	0	600	1700	1700	600	1700	600	300
18	100	100	200	500	600	0	300	400	100	300	100	0
19	300	300	800	1300	1700	300	0	1200	400	1200	300	100
20	600	500	1100	1600	1700	400	1200	0	1200	2400	700	400
21	600	400	800	600	600	100	400	1200	0	1800	700	500
22	1300	1200	2600	1200	1700	300	1200	2400	1800	0	2100	1100
23	800	1100	1000	500	600	100	300	700	700	2100	0	700
24	700	400	400	300	300	0	100	400	500	1100	700	0